NASA CR 121165
W268-73-1

FINAL TECHNICAL REPORT

RESEARCH INTO THE FEASIBILITY OF THIN METAL- AND OXIDE-FILM CAPACITORS

by
G. V. Jorgenson
and
H. W. Larson

June 1973

Prepared Under Contract No. NAS 3-14373 by

NORTH STAR RESEARCH AND DEVELOPMENT INSTITUTE
3100 THIRTY-EIGHTH AVENUE SOUTH • MINNEAPOLIS, MINNESOTA 55406

Lewis Research Center
NATIONAL AERONAUTICS AND SPACE ADMINISTRATION

1. Report No.	2. Government Accession No.	3. Recipient's Catalog No.
NASA CR 121165		

4. Title and Subtitle	5. Report Date
FINAL TECHNICAL REPORT ON RESEARCH INTO THE FEASIBILITY OF THIN METAL- and OXIDE-FILM CAPACITORS	June 1973
	6. Performing Organization Code
7. Author(s) G.V. Jorgenson and H.W. Larson	8. Performing Organization Report No. W-268-73-1
	10. Work Unit No.
9. Performing Organization Name and Address North Star Research and Development Institute 3100 Thirty-Eighth Avenue South Minneapolis, Minnesota 55406	11. Contract or Grant No. NAS3-14373
	13. Type of Report and Period Covered Contractor Report May 1971 - December 1972
12. Sponsoring Agency Name and Address National Aeronautics and Space Administration Lewis Research Center 21000 Brookpark Road Cleveland, Ohio 44135	14. Sponsoring Agency Code

15. Supplementary Notes

Project Manager, James A. Kish, Spacecraft Technology Division, NASA-Lewis Research Center, Cleveland, Ohio

16. Abstract

Thin film capacitors with up to twenty-two active layers have been deposited by RF sputtering. The materials were aluminum electrodes of 1200 to 1500 angstrom thickness and silica dielectric layers of 3000 to 6000 angstrom thickness. The best electrical characteristics were capacitances of nearly 0.1 microfarad for an active area of 1.25 square centimeters, dissipation factor of less than 0.01 over a frequency range of 0.5 to 100 kilohertz and energy density of approximately 70 millijoules per cubic centimeter of active deposited material at a working voltage of 40 volts. These aluminum-silica capacitors exhibit excellent electrical stability over a temperature range from -55°C to +300°C.

17. Key Words (Suggested by Author(s))	18. Distribution Statement
Capacitors Thin Films Sputtering	Unclassified - unlimited

19. Security Classif. (of this report)	20. Security Classif. (of this page)	21. No. of Pages	22. Price*
Unclassified	Unclassified	40	$3.00

* For sale by the National Technical Information Service, Springfield, Virginia 22151

Page Intentionally Left Blank

TABLE OF CONTENTS

FINAL REPORT
May 1971 through December 1972

on

RESEARCH INTO THE FEASIBILITY OF THIN METAL- AND OXIDE-FILM CAPACITORS

Prepared for

NASA-Lewis Research Center, Cleveland, Ohio 44135
Under Contract No. NAS 3-14373

by

North Star Research and Development Institute
3100 Thirty-Eighth Avenue South, Minneapolis, Minnesota 55406

June 1973

Summary

This report summarizes the results of a twenty-month research program to investigate the feasibility of producing high-energy-density, high-temperature, multilayer thin-film capacitors using a radio frequency (rf) sputtering technique. This program is a continuation of an investigation performed by North Star Research and Development Institute under Contract NAS 12-551. The results of that study are presented in the final report (Reference 1).

The research efforts carried out under Contract NAS 3-14373 have resulted in the development of capacitors having up to 22 active capacitor layers; *i.e.*, 22 quartz dielectric layers alternated with 23 layers of aluminum electrodes. The electrode and dielectric thicknesses are approximately 1500 and 6000 angstroms (Å), respectively. Some of the best values of electrical characteristics for the test capacitors are as follows:

- Capacitances of nearly 0.1 microfarad for an active area of 1.25 square centimeters;
- Energy densities of approximately 70 millijoules per cubic centimeter of active deposited material at a working voltage of 40 volts. Generally, these capacitors were not tested at more than 40 volts, but had 6000 Å-thick dielectric layers and would probably operate reliably at 100 volts where their energy densities would be 175 millijoules per cubic centimeter;

- Dissipation factors of less than 0.01 over a frequency range of 0.5 to 100 kilohertz.

The early capacitor development efforts carried out on the previous program (Contract No. NAS 12-551) indicated that multi-layer capacitors composed of aluminum electrodes and quartz dielectrics that would operate well at temperatures from -55°C to +300°C and at frequencies up to 100 kilohertz could be produced. A ten-layer capacitor was deposited and indications were that with improvements in the equipment, capacitors having up to twenty layers or more would be possible. As a first step in upgrading the equipment, a mask- and target-changer assembly was fabricated. However, it could not be put into use before the program ended. This assembly was installed in the vacuum system during the subject contract period and several modifications were made to improve its operation. Using this mask- and target-changer, electrode-dielectric combinations can now be deposited without breaking vacuum.

The principal problem with depositing multilayer capacitors using this system has been the continuing presence of minor defects (shorts or low-resistance paths through the dielectric). These defects can be healed by applying d.c. potential to the capacitors. Modification of the system made this healing possible in the vacuum system by having electrical connection to each capacitor as it was being fabricated. These connections also made it possible to check capacitance, dissipation factor, and leakage current after each deposited capacitor layer.

The improvements in the equipment have resulted in considerable savings in the total time required to deposit a multilayer capacitor. Of equal importance is the good electrical performance of the devices. Detailed descriptions of the test equipment and procedures, along with a discussion of the test results, are presented in the following sections of this report.

INTRODUCTION

The National Aeronautics and Space Administration has a requirement for capacitors with performance capabilities superior to those now available. Some of the requirements are high capacitance per unit volume, low power dissipation, and a high degree of electrical and mechanical stability over wide temperature and frequency ranges. These sometimes conflicting requirements can best be satisfied by a capacitor consisting of many stacked and parallel-interconnected pairs of electrodes and dielectrics. All capacitors were fabricated with aluminum electrodes of approximately 1500 Å thickness and quartz dielectrics of 3000 to 6000 Å thickness.

The bulk dielectric constant for quartz is 3.75, and that for the sputter-deposited thin films is slightly less (usually about 3.2 to 3.6). For a material of any given dielectric constant, the capacitance per unit volume of a single-layer capacitor can be increased by decreasing the thickness of the deposited films. The thinner layers give lower mass and volume for a given number of layers, and a thinner dielectric gives increased capacitance per layer. The limit to which the thickness of the dielectric can be decreased depends on the voltage that the capacitor must hold without breaking down. If the voltage requirements are very low (less than approximately 25 volts) thickness becomes limited by problems in manufacturing. As the dielectric becomes very thin, an increasing percentage of the capacitors have shorts, and the yield decreases. This usually occurs at dielectric thicknesses below 2000 Å. The limit to which the electrode thickness can be decreased is governed by the conductivity of the electrode material. The sheet resistance of the electrodes must be kept very low to have capacitors with low power dissipation.

RF sputtering was used for the deposition of all dielectric films in this program. The principal advantage of rf sputtering the bulk dielectric material for capacitor dielectrics rather than anodizing (Reference 2), vacuum evaporating (Reference 3), or reactively sputtering (Reference 4), is the capability of depositing a film with the same stoichiometry as the target material. RF sputtering also produces films of high density with good adhesion, and allows precise control of deposit thickness.

The principal problem encountered in performance of this contract was the presence of defects such as small shorts. Although these can be healed in a single-layer capacitor, the problem becomes more difficult when healing individual layers of a multilayer capacitor. The primary source of the defects is particulate matter generated in the vacuum chamber by deposits that craze and fall off the various surfaces on which they collect. Many modifications were made to improve this situation while staying with the basic deposition system. Redesign of the system would allow even greater improvement in the deposition process.

A survey of the capabilities of various commercially available capacitors was given in the Final Technical Report on Contract NAS 12-551 (Reference 1). Reported in the same document are the excellent characteristics of aluminum-quartz capacitors having only a few layers--in most cases, two. In the present contract, capacitors of up to 22 layers have been deposited. With further progress toward eliminating defects caused by particulate matter, it is expected that the excellent characteristics referred to above can be combined with the multilayer capability to produce capacitors that meet the NASA's rigid requirements.

EXPERIMENTAL WORK

Capacitors were made by alternate rf sputter deposition of quartz dielectric layers and aluminum electrode layers on thin glass substrates. The sputtering was performed in an ultrahigh vacuum system in North Star's cleanroom facility. The aluminum electrode layers were stacked such that the even-numbered layers were identical and electrically connected; the same was true for the odd-numbered electrode layers. A dielectric layer separated each even- and odd-numbered electrode, producing a parallel array of capacitors with high energy-storage density.

Capacitors were tested for capacitance and dissipation factor as functions of frequency and temperature and also for d.c. leakage current.

Equipment

Vacuum System

All rf sputtering was done in an Ultek 18-inch-diameter ultrahigh vacuum system. This system utilizes cryosorption pumping for roughing and titanium sublimation and ion pumping for high vacuum. The system is fitted with a 6-inch-high glass cylinder and a stainless steel top plate with a center hole through which the rf electrode projects. Figure 1 shows the system in North Star's cleanroom facility.

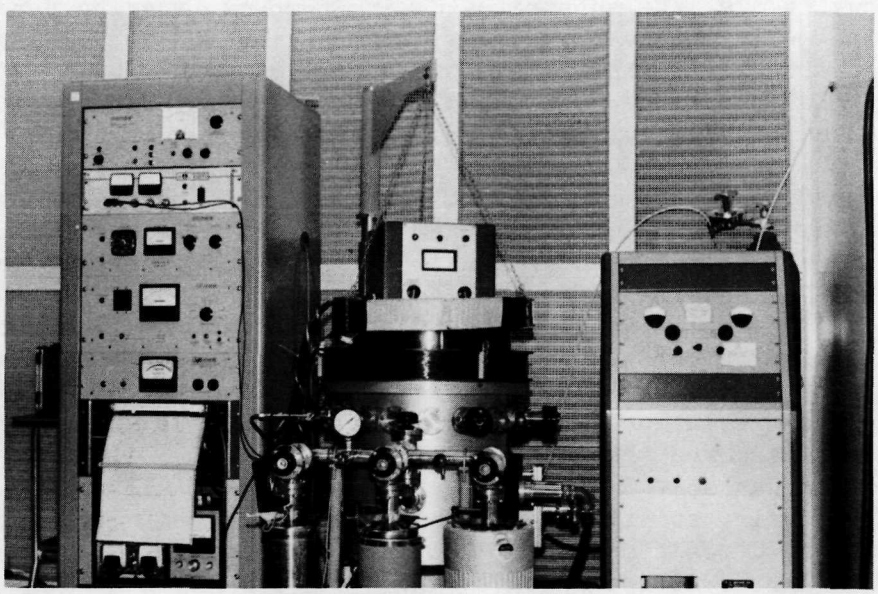

Figure 1. Sputtering System in North Star's Cleanroom

A consolidated Vacuum Corporation CVE-14 vacuum evaporator was used for depositing narrow bands of aluminum to two opposite edges of each substrate. These deposits were used for attachment of the gold connecting leads.

Sputtering Module

The rf sputtering was performed with an R.D. Mathis Company, Model SP 310, sputtering module (refer to Figure 1). The cabinet, shown at the right, is a 13.56 MHz, 1.0 kw transmitter designed to feed a 50-ohm load. The tuning unit is shown atop the vacuum chamber. Its function is to tune the load to 50 ohms for maximum coupling of power into the sputtering target. Two electromagnets, consisting of large coils of wire, are arranged concentrically around the vertical axis of the sputtering chamber. The magnetic field produced by the electromagnets increases the rf plasma density and keeps the plasma contained in the immediate vicinity of the target.

Mask-and-Target Changer

A mask-and target-changer assembly had been designed and fabricated on the previous program (NAS12-551), but it had not been tested. Figure 2 shows four capacitors on the substrate table with the mask disk in each of its four positions. One position is a port for loading and unloading substrates. The three sets of masks are for the two electrode configurations and the dielectric. The loading-unloading port has a cover that acts as a close-fitting shutter over the substrates during pumpdown, during target stabilization, and while the quartz target is being moved. The aluminum target is mounted directly on the rf electrode and is centered above the substrate table. For quartz deposition, a flat quartz plate is moved into place very close to the aluminum target and completely covering it.

During the performance of the subject contract, many modifications were made to the mask-and-target changer. A new substrate table was built that incorporated eight electrical feedthroughs. This provided contacts for the gold wires so that the healing of defects and testing could be carried out in the vacuum system. The gold leads on the substrates also required another modification. Earlier in the program, the mask disk had operated close to the substrate surfaces. Use of the one-mil gold leads, plus the necessity of maintaining a required clearance above the wires, would have caused excessive spacing between the mask and the substrate, resulting in poorly defined deposit edges. This problem was solved by adding a mechanism that allows the mask table to be lifted during rotation and then lowered such that it rests on the gold wires during deposition. This manipulation is carried out through the use of a push-pull linear-motion feedthrough.

Mask disk rotation and movement of the quartz target are accomplished through rotary-motion feedthroughs. In the original configuration, the

(a)

(b)

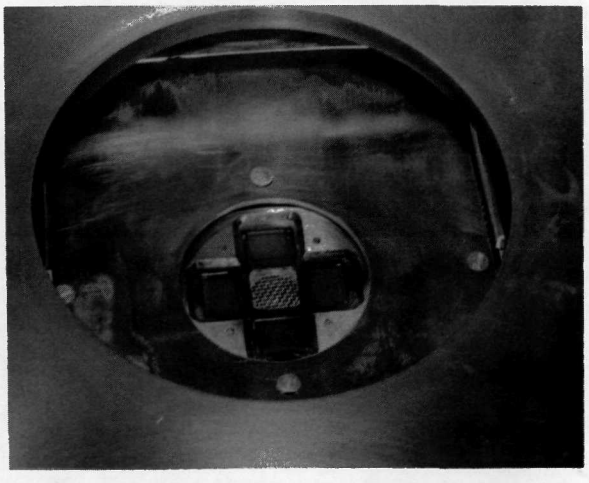

(c)

(d)

Figure 2. Capacitors on Substrate Table as Seen from Above the Vacuum Chamber. The Mask Disk is in Four Positions: (a) Loading-Unloading, (b) Electrode Deposition, (c) Dielectric Deposition, (d) Counter-Electrode Disposition

rotary motion for the target changing was converted to linear motion through a system of gears. The quartz target was attached to two racks that moved in rails as shown in Reference 1, page 11. This configuration was changed because the mechanism collected large amounts of sputtered material and the sliding of the racks in the rails kept loosening these deposits. All the components of the target changer above the main support plate were removed except for one rotary shaft that comes through the plate. The quartz target is clamped to this shaft so it can be rotated into and out of position for sputtering. The arrangement is shown in Figure 3. This modification greatly reduced the density of loose particulate matter in the system.

Deposit Thickness Monitor

A Sloan Technology Corporation Model DTM-3 Deposit Thickness Monitor was used for controlling the deposits to the desired thickness. The sensing element is a 5 MHz quartz crystal. A variable-frequency oscillator is tuned to the frequency of the crystal and the mass of the crystal increases during deposition. The resultant beat frequency is calibrated to deposited film thickness. The original crystal oscillator that was supplied with the instrument was unsatisfactory for use in a 13.56 MHz environment (the rf plasma). Sloan developed a new sensing head for use in sputtering environments and North Star acquired one of these during June 1971. Sloan stated that the new monitor head could accurately measure deposited thickness only when the plasma was turned off. Thus, it was first thought that it would be necessary to periodically stop the sputtering and turn on the deposit thickness monitor to measure the deposit. Then the monitor would have to be disconnected and the sputtering resumed. Use of the system in this manner would have resulted in considerable delay in order to avoid making the thickness measurement at the time of greatest temperature drift in the system. However, the monitor was found to be capable of operating during sputter deposition when properly shielded. Two meshes were placed between the monitor head and the substrate table and spaced apart less than the Langmuir dark space thickness. The upper mesh was in contact with the substrate table and can be seen in the center hole of the substrate table in all four views of Figure 2. Both meshes were electrically grounded. These meshes reduced the sensitivity of the monitor because of having a transmittance of approximately 50 percent. However, all films deposited on this program were thick enough that the 50 percent loss of material was not important and accuracy was not adversely affected by insertion of the meshes. Other meshes were arranged around the monitor head to prevent any plasma contact with the head. These precautions made continuous monitoring during deposition possible. Figure 4 shows a typical recorder trace of frequency change versus time as films are being deposited. The CW and CCW refer to rotation of the mask disk feedthrough for the two different electrode patterns. The notations, #2 and #3, refer to the capacitor layer number completed with that aluminum deposition. Every few weeks the monitor began to make 30 to 40 Hz shifts, apparently between two modes of oscillation. This signaled that a new crystal was needed. The present configuration works very well and provides film thickness control that meets or exceeds the 10 to 15 percent requirement of the contract.

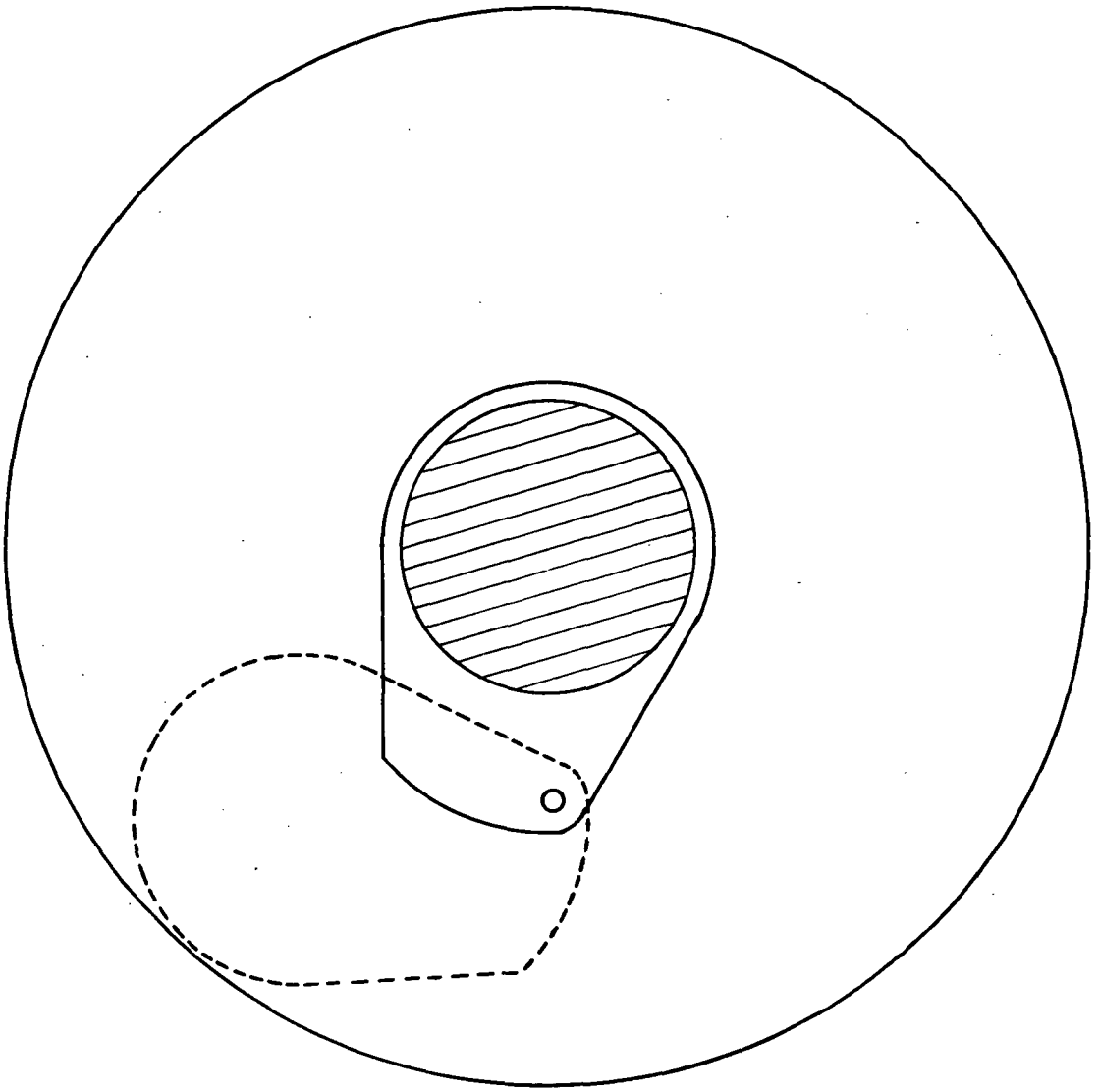

Scale = 1/3 actual

Figure 3. Vertical View of the New SiO_2 Target in Position for SiO_2 Deposition (Solid Line) and for Aluminum Deposition (Dashed Line); Crosshatch Shows the Aluminum Target

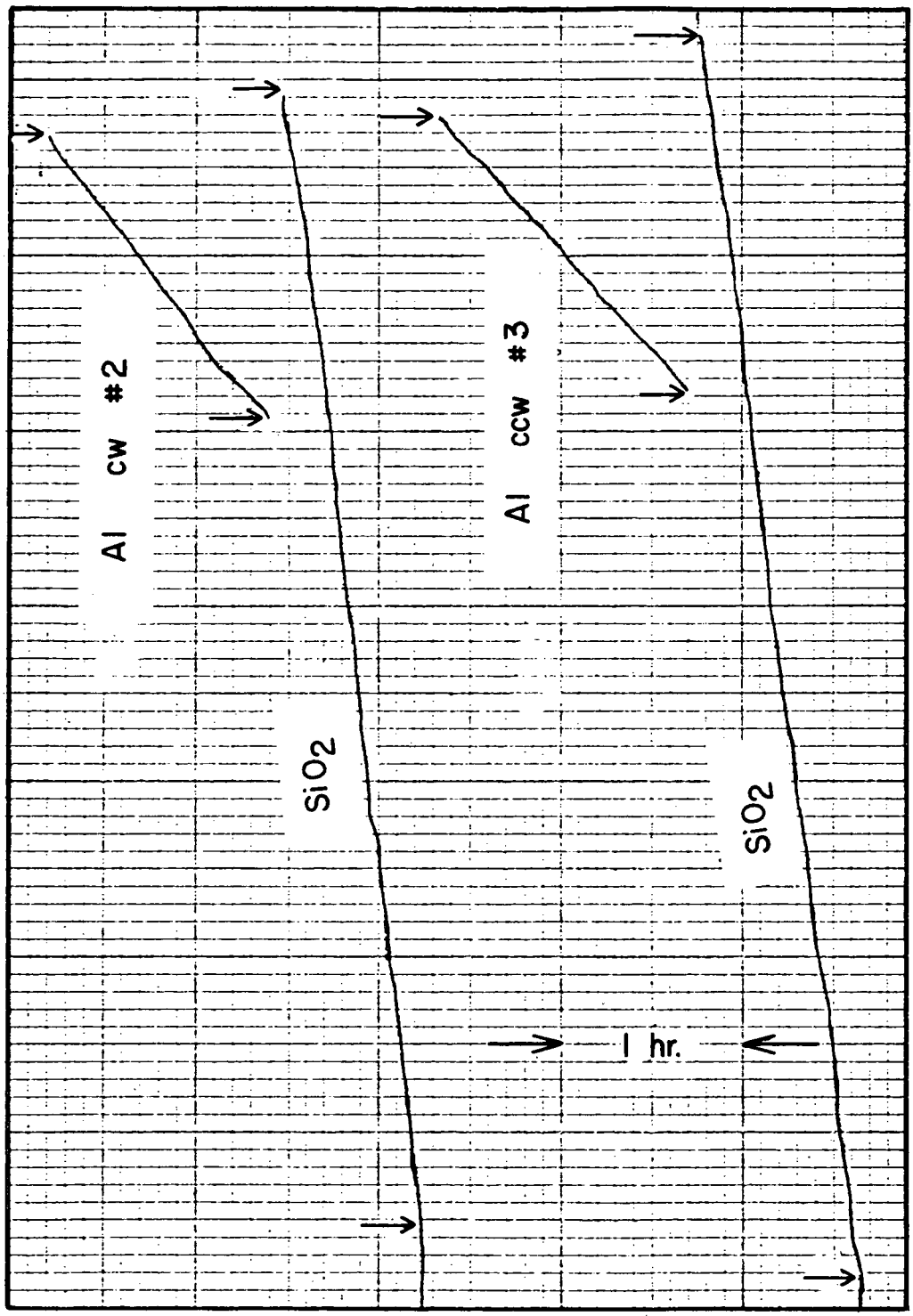

Figure 4. Recorder Trace of Frequency from Thickness Monitor versus Time during SiO_2 and Aℓ Depositions

Capacitor Test Equipment

The test circuit for capacitance and dissipation factor measurement consisted of a General Radio Type 1615A capacitance bridge and an audio generator. The frequency capability of the system is 200 Hz to 100 kHz. The equipment was connected directly to a junction box, which, in turn, was connected to the substrates in the vacuum system. The test setup was portable so it could be moved to an oven containing a test block for supporting the capacitors during high-temperature tests.

Capacitor Fabrication

Substrate Preparation

Several substrate cleaning techniques were investigated during the course of this program. The following cleaning schedule was selected and used for the majority of the work:

- Ultrasonic agitation in a detergent solution for a minimum of five minutes;
- Hot tap-water rinse;
- Ultrasonic agitation in deionized water;
- Methanol spray rinse;
- Ultrasonic agitation in methanol; and
- Drying in an argon jet.

After treatment the substrates were ready for the vacuum evaporation of the aluminum strips and the bonding of the gold leads. The aluminum strips were approximately one millimeter wide at opposite edges of the substrates. One-by five-mil gold wires were attached to these deposits by thermocompression bonding. Figure 5 shows a 19-mm square substrate with gold leads attached. During the bonding operation, the substrates were handled only with tweezers and the work was carried out in a clean bench. The substrates were then stored in a clean container until ready for use. At that time they were ultrasonically agitated in methanol, dried in an argon jet, and placed on the substrate table.

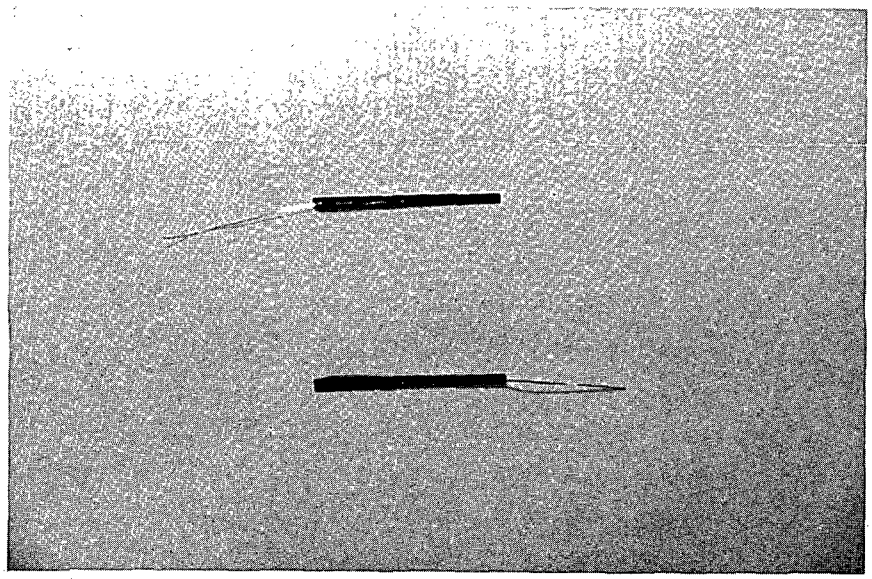

Figure 5. Capacitor Substrate with Gold Wires Attached

Deposition Parameters

Several attempts were made at increasing the deposition rates for both aluminum and quartz to decrease the time required for fabrication. The geometry of the deposition system appears to limit the deposition rate for good aluminum films (those exhibiting specular reflection of incident light). When the substrates are too hot, the depositing aluminum forms large crystallites, resulting in a rough, non-specularly reflecting surface. In the present system, the only way to limit the temperature rise is to run at relatively low rf potential (approximately 475 volts) resulting in a deposition rate of 25 to 30 Å per minute. The deposition rate of quartz was found to be related to the space between the quartz and the aluminum targets (see description of system under heading "Mask-and-Target Changer"); the rate becomes higher as the space is reduced. Typical rates for quartz deposition have been approximately 60 to 65 Å per minute at an rf potential of 1050 volts when operating with a quartz-to-aluminum spacing as small as practicable.

A relatively large number of the first capacitors fabricated with the mask-and-target changer were shorted. It appeared that one reason for this problem was because of trying to use the maximum amount of the substrate surface. Small amounts of aluminum (from slightly feathered edges) from the two electrode patterns were shorted together. The two electrode patterns were also of the

same width, so edges of the electrodes became coincident. This would probably have given more trouble, becoming a very high stress area, when depositing multilayer capacitors. A new mask was fabricated for one of the electrodes, making it slightly smaller than the other electrode. This change eliminated the shorting by mutual contact of the deposits through the two electrode masks. Also, in later multiple layer depositions, there was no indication of failure along the edges of the aluminum deposits. The need for modifications in the system, such as those that have been discussed, was found by depositing many two-, three-, and four-layer capacitors.

Although many mechanical problems were encountered during the program, one of the most serious was warpage of the substrates, which caused them to catch in the mask changer when it was rotated. The substrates used during the early part of the program were 50- to 85-micron-thick glass. Alternate heating and cooling caused these substrates to warp. Annealing greatly reduced the warpage problem, but to reduce the warpage even further, and to allow easier handling, thicker substrates (160 to 190 microns) were used. It was decided that substrate mass could be reduced after solving the more pressing problem of establishing the number of layers that could be deposited to give high performance capacitors.

Minor shorts and low-resistance paths were healed by the application of a d.c. potential (Reference 1, page 24). After depositing three to five layers, there were often too many shorts to heal by this technique. If defects in layers other than the top layer did heal, the energy release was often great enough to destroy the capacitor. This led to the conclusion that defects in each layer must be healed before the next layer was deposited, as was done before the mask- and target-changer system was used. An eight-pin electrical feedthrough was installed to provide electrical contact to both electrodes of all four substrates. A new substrate table was fabricated with spring-loaded electrical contacts that accommodate 1.0 by 5.0 mil gold leads, which are thermocompression bonded to aluminum deposits on the substrates (Figure 5). With this arrangement, a dc potential could be applied to each substrate after every capacitor layer had been deposited. The capacitor healing was done under the limitation of 4.0 mA maximum current unless a certain substrate would not heal at that current level. This current limitation reduced the energy that was dissipated when healing took place and prevented the energy release from damaging the capacitor.

Several multilayer capacitors were made by healing the defects under different environmental conditions. Healing defects in vacuum and in air differ in two important ways: 1) there is no convective cooling to carry away the heat generated by electrical conduction through the defect during the healing procedure; and 2) there is no oxygen available for oxidation of the aluminum that becomes hot from conduction through the defect.

Some capacitors were made by raising the pressure to about 0.8 atmosphere of argon to provide convective heat loss mechanisms during healing without

providing oxygen. There was no noticeable difference between these capacitors and those healed in vacuum.

Some capacitors were fabricated by introducing approximately 100 Torr of air into the system for the healing. This provided approximately 20 Torr of oxygen, which is sufficient for oxidation of thin aluminum conducting paths when they become hot during healing. This procedure also produced no noticeable difference from healing in vacuum.

A further modification in the healing process reduced the chances of damaging the capacitors even further. This entailed the charging of another capacitor and then discharging that capacitor through each of the thin-film capacitors. The capacitance of this capacitor and the charging potential can be controlled for utmost protection of the deposited capacitors.

Capacitors that were fabricated by opening the vacuum system to change sputtering targets and by removing them from the system after each capacitor layer for healing, continued to have many defects on each successive layer (Reference 1). Originally, it was thought that the excessive handling was the cause of the defects. Therefore, it was anticipated that with the present arrangement of mask-and-target changing and *in situ* healing, the number of defects to be healed would greatly diminish after the first layer or two. However, that was not the case, indicating that the defect-producing mechanism was present throughout a multilayer deposition. Dust generated in the system by flaking of deposits from various surfaces was suspected as the most likely source of the defects. This dust would drift around in the system every time the vacuum system was evacuated and brought up to air. Even though the top of the system was cleaned each time it was open, the large volume below the main support plate for the mask-and-target changer was largely inaccessible. It appeared that the best proof that particulates in the system were the cause of the defects was to completely clean the entire system. Then, at least immediately after the cleaning, the defect density should be much lower.

The mask-and-target changer assembly was removed from the vacuum chamber and completely disassembled. All surfaces that had received deposited quartz and aluminum were thoroughly cleaned, using silicon carbide abrasive paper and chemical etching. This was followed by methanol rinsing and blowing dry with clean argon. The sublimated titanium inside the walls of the vacuum chamber was also removed using abrasive paper. After reassembling, aluminum was sputter deposited on all three mask-containing segments of the mask disk. This was necessary because if quartz is deposited directly on any part of this disk, the film will begin to peel off much sooner. All the capacitors with 15 to 21 active layers were deposited after this cleanup. The density of spots where defects had been healed was noticeably lower than before and there were no large defects as had appeared before the cleanup. Because of limited available time, the dielectric thickness was increased to 5000Å at the same time that the cleanup was made. This was done to increase the probability of obtaining multilayer capacitors.

Smaller-area capacitors were fabricated in an attempt to relate failure and defect density. These capacitors had areas of approximately one-fifth and one-eighth of the other capacitors reported here. They also had 1500 Å-thick electrodes and 6000 Å-thick dielectrics. The program ended before these could be carried on to a large number of layers (eight layers maximum) but all the capacitors of this size had excellent electrical characteristics. The last group of four capacitors was brought to eight layers with no healing and testing after each layer. They were removed from the system and healed. Although there were many shorts, three of the units became excellent capacitors after healing; this had not been possible on the larger-size capacitors with no healing for eight layers. Dissipation factors were well below 0.005 at all frequencies up to 20 kilohertz and less than 0.01 at all frequencies tested and at temperatures up to 250°C. These results are very encouraging and indicate that, if the area of deposited capacitors is limited to something less than one square centimeter and the geometry of the deposition chamber is designed for limiting particulate contamination, these capacitors can be far better than those currently available.

Capacitor deposition begins by initiating a rf plasma with the mask disk positioned such that the substrates are shielded. The system is allowed to operate until equilibrium is reached--no further drift in the settings of the rf tuning unit. This is basically a thermal equilibrium problem, requiring at least ten minutes. The mask disk is rotated and lowered to begin the first electrode deposition. This usually disturbs the equilibrium slightly and the system must be re-tuned. The aluminum deposition process is monitored using the quartz-crystal system (see Figure 4) until the paper thickness is achieved. When the desired film thickness has been reached, the mask disk is raised and rotated to again shield the substrates. The quartz target is moved into place and the rf power tuned to the new load. The quartz has to sputter for approximately twenty minutes to reach thermal equilibrium and to remove possible contamination that reaches the front surface of the quartz during aluminum deposition. The mask change is made and after the quartz deposition, the procedure is repeated--mask change to shutter position, target change, re-tune, ten minute sputtering to reach equilibrium on the aluminum, and mask change. The time line for this sequence is shown in Figure 6a. Figure 6b shows how the sequence is modified when each layer is healed and tested. The plasma is turned off after each aluminum layer, beginning with the second. One hour is allowed for the system to reach thermal equilibrium before testing. After the test, the plasma is reignited and operated for twenty minutes before the next quartz deposition begins.

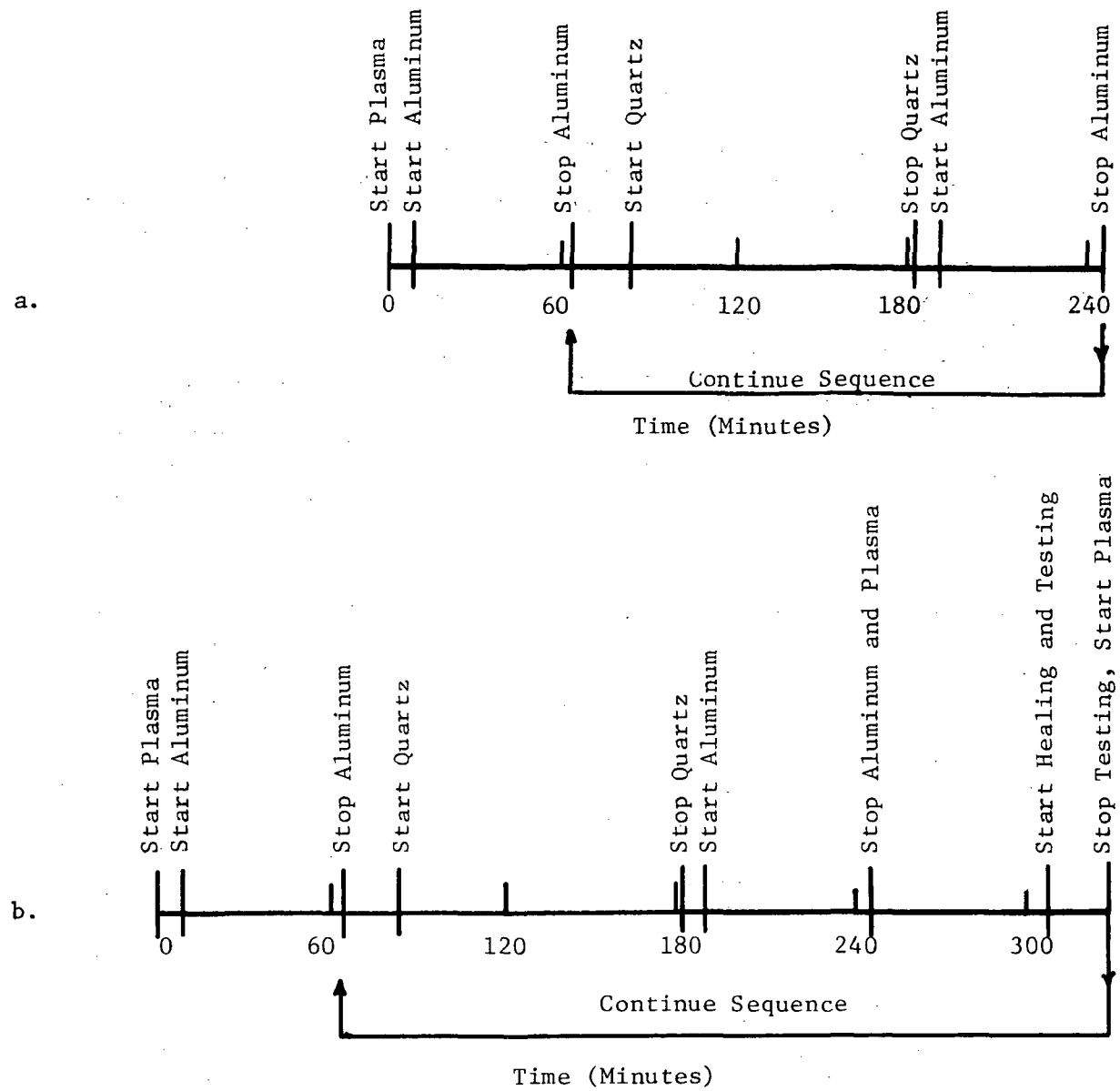

Figure 6. Time Sequence for Capacitor Deposition:
a. Without Healing and Testing, and
b. With Healing and Testing of Each Layer.

Capacitor Test Results

Many capacitors of up to four layers were fabricated early in the program. The fact that they appeared to be limited to approximately four layers was the basis for the many system modifications that have been discussed in the foregoing sections of this report. Figure 7 shows the capacitance as a function of frequency at three temperatures for a typical four-layer capacitor. The dissipation factor as a function of the same parameters is presented in Figure 8. These temperature-dependent electrical characteristics were stabilized by baking the capacitors in air at temperatures of at least 300°C. The quartz layers in these capacitors were approximately 3500 Å thick and the aluminum electrodes were 1500 Å thick. Energy densities for these capacitors were approximately 60 millijoules per cubic centimeter of deposited material.

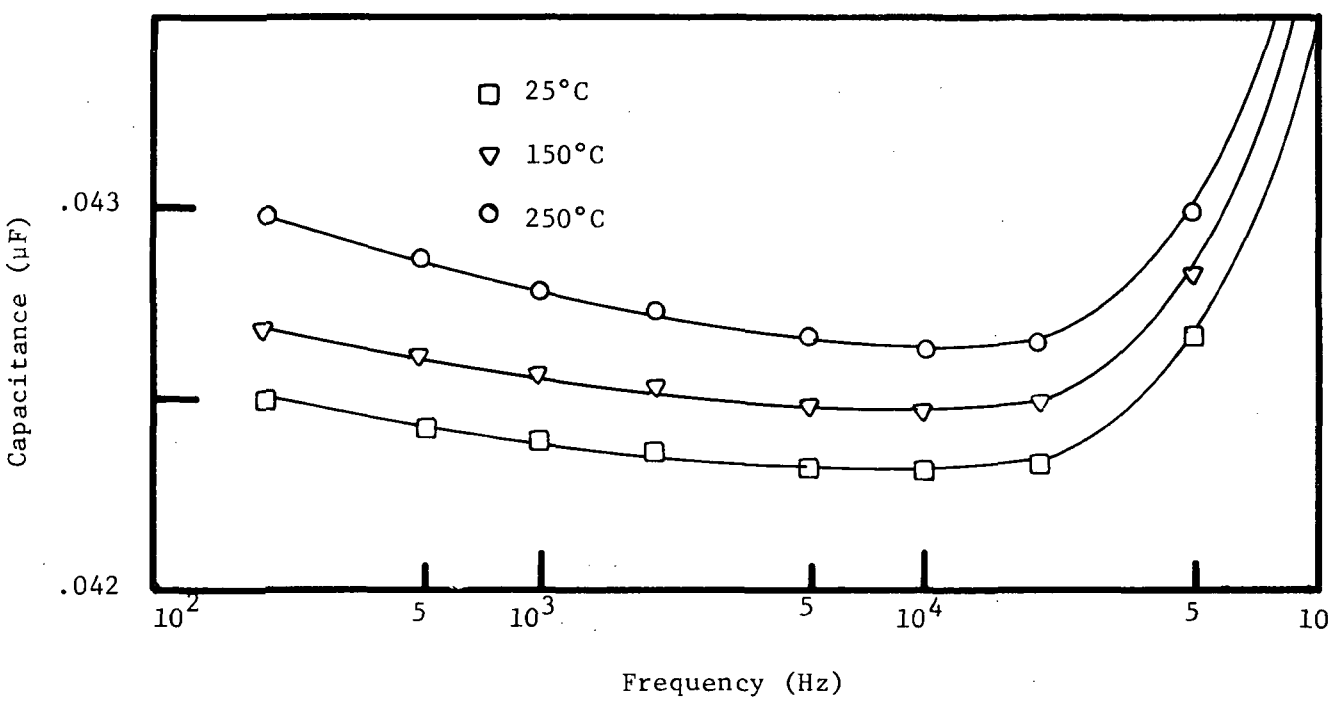

Figure 7. Capacitance as a Function of Frequency for a Four-Layer Silica-Aluminum Capacitor at Three Temperatures.

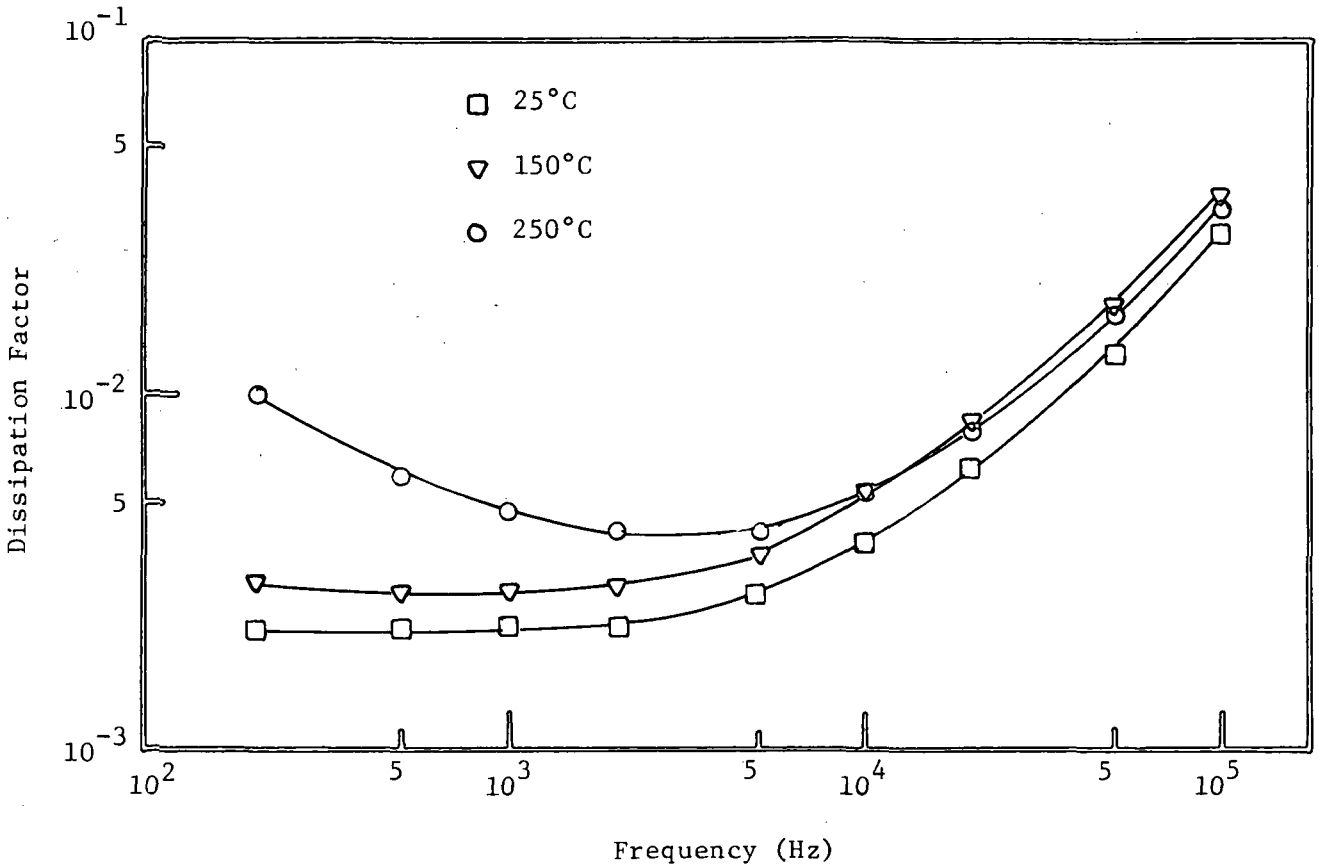

Figure 8. Dissipation Factor as a Function of Frequency for a Four-Layer Silica-Aluminum Capacitor at Three Temperatures

Table 1 is included to show actual test data from a run using *in situ* healing and testing of the capacitors. This run resulted in three useful five-layer capacitors. A contact to one of the substrates was lost before the first layer could be tested, but the other three had test results that were typical for all the capacitors made in this way before the complete system cleanup. The run was terminated after five layers because resistance before healing became low, and the healing current requirements became high.

Particulate density in the vacuum system decreased many fold as a result of the complete cleaning of everything inside the vacuum chamber. Substrates that went through several pump-down and up-to-air cycles had essentially no visible particulates on them. This compared to the previous condition wherein particles were visible to the unaided eye. Visually, the defect density immediately after the cleanup was estimated to be at least two orders of magnitude lower than before. As stated earlier, dielectric layers were increased in thickness to 5000 Å at this same time.

Table 1

Resistance Before Healing, Maximum Current During Healing, and Dissipation Factor and Capacitance at 1.0 kHz After Healing for One Run of Four Substrates

Capacitor Layer Number	Substrate Number	Resistance (Ohms)	Maximum Current Conducted (mA)	Dissipation Factor After Healing	Capacitance After Healing (pF)
1	1	$>10^9$	1×10^{-2}	8×10^{-3}	8,000
	2	5×10^3	2×10^{-1}	3.5×10^{-3}	6,430
	3	4×10^6	1×10^{-2}	4.4×10^{-3}	8,160
	4	$>10^9$	$<2 \times 10^{-4}$	Not Connected	
2	1	short	2×10^2	3×10^{-3}	16,430
	2	$>10^9$	3.5×10^{-2}	2.3×10^{-3}	13,440
	3	short	3×10^2	2×10^{-3}	17,060
	4	$>10^9$	--	--	--
3	1	$>10^9$	4×10^{-1}	1.7×10^{-1}	25,910
	2	40	3	1×10^{-2}	20,100
	3	$>10^9$	6×10^{-2}	2×10^{-3}	26,130
	4	--	--	--	--
4	1	$>10^9$	1×10^{-1}	1.4×10^{-1}	30,460
	2	$>10^9$	8.5×10^{-2}	4×10^{-1}	27,400
	3	$>10^9$	2.5×10^{-2}	2×10^{-3}	31,020
	4	--	--	--	--
5	1	2.3×10^5	2×10^{-1}	2.6×10^{-3}	37,420
	2	1×10^4	10	1.9×10^{-3}	30,470
	3	7×10^3	3×10^{-1}	3.8×10^{-3}	38,910
	4	--	--	--	--

A number of mechanical problems were encountered during the early part of the first run after cleanup, requiring that the system be opened many times. Even so, the first two capacitors that failed on this run, failed after eight layers. Their capacitances were 0.0466 and 0.0413 microfarads, with dissipation factors of 0.007 and 0.36, the latter being up from 0.016 after the previous layer. This run was terminated after the sixteenth layer when the third failure occurred. The final values for capacitance and dissipation factor of the sixteen-layer capacitor were 0.06 microfarads and 0.002, respectively, as measured in the vacuum system at 1.0 kilohertz and approximately 25°C. This capacitor was removed from the vacuum system and tested in air. Figure 9 shows its capacitance as a function of frequency at four temperatures ranging from 25° to 150°C. This capacitor failed during the testing so it is not known if the temperature effects as shown are reversible. The dissipation factor

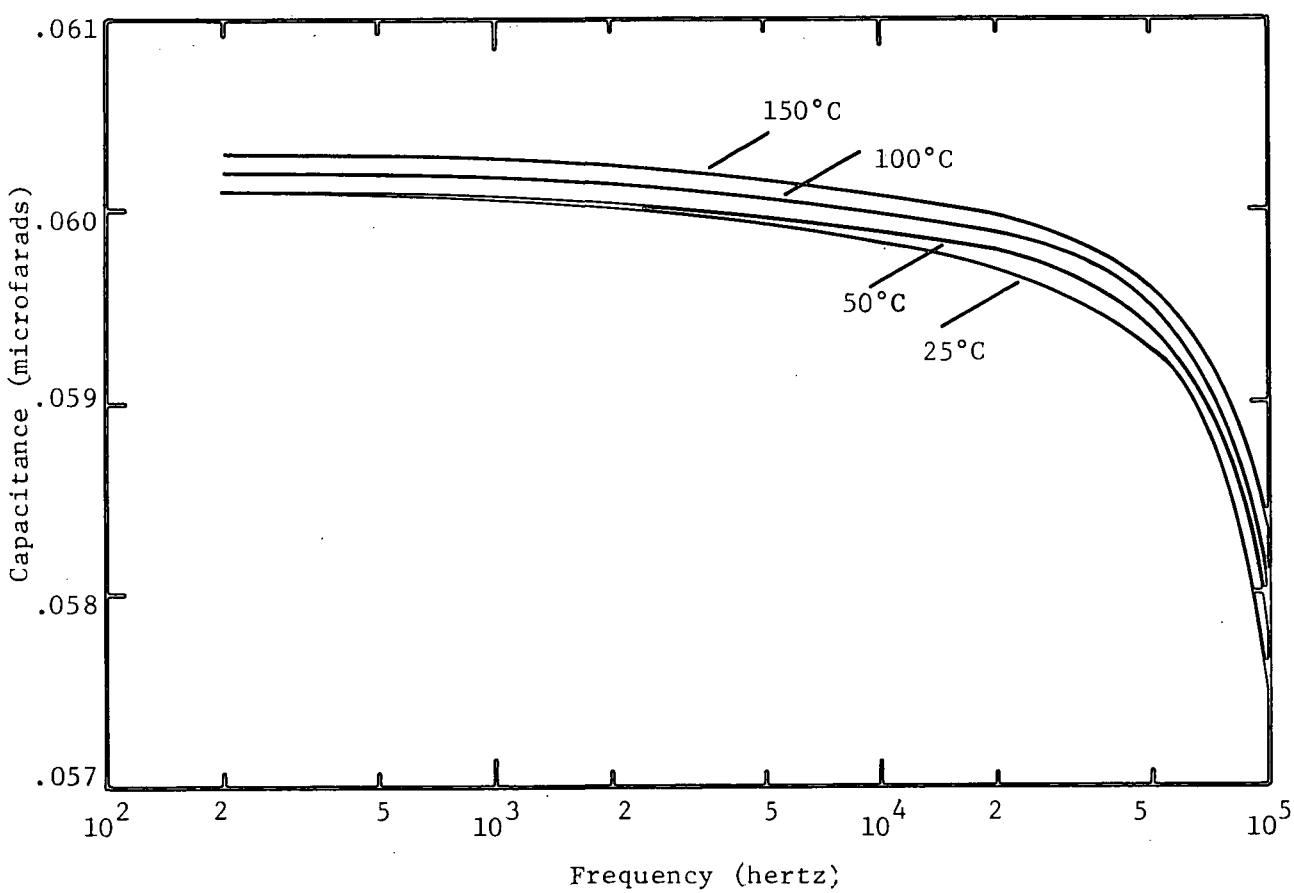

Figure 9. Capacitance as a Function of Frequency at Four Temperatures for a Sixteen-Layer SiO_2-Al Capacitor

measurements indicated that the thermal effects probably were not reversible because annealing apparently was taking place at temperatures as low as 50°C. Figure 10 shows the dissipation factor-frequency curves. The 25°C data yielded a smooth curve with high stability. At 50°C and at 100°C, the dissipation factor readings were very unstable, indicating that change was taking place in

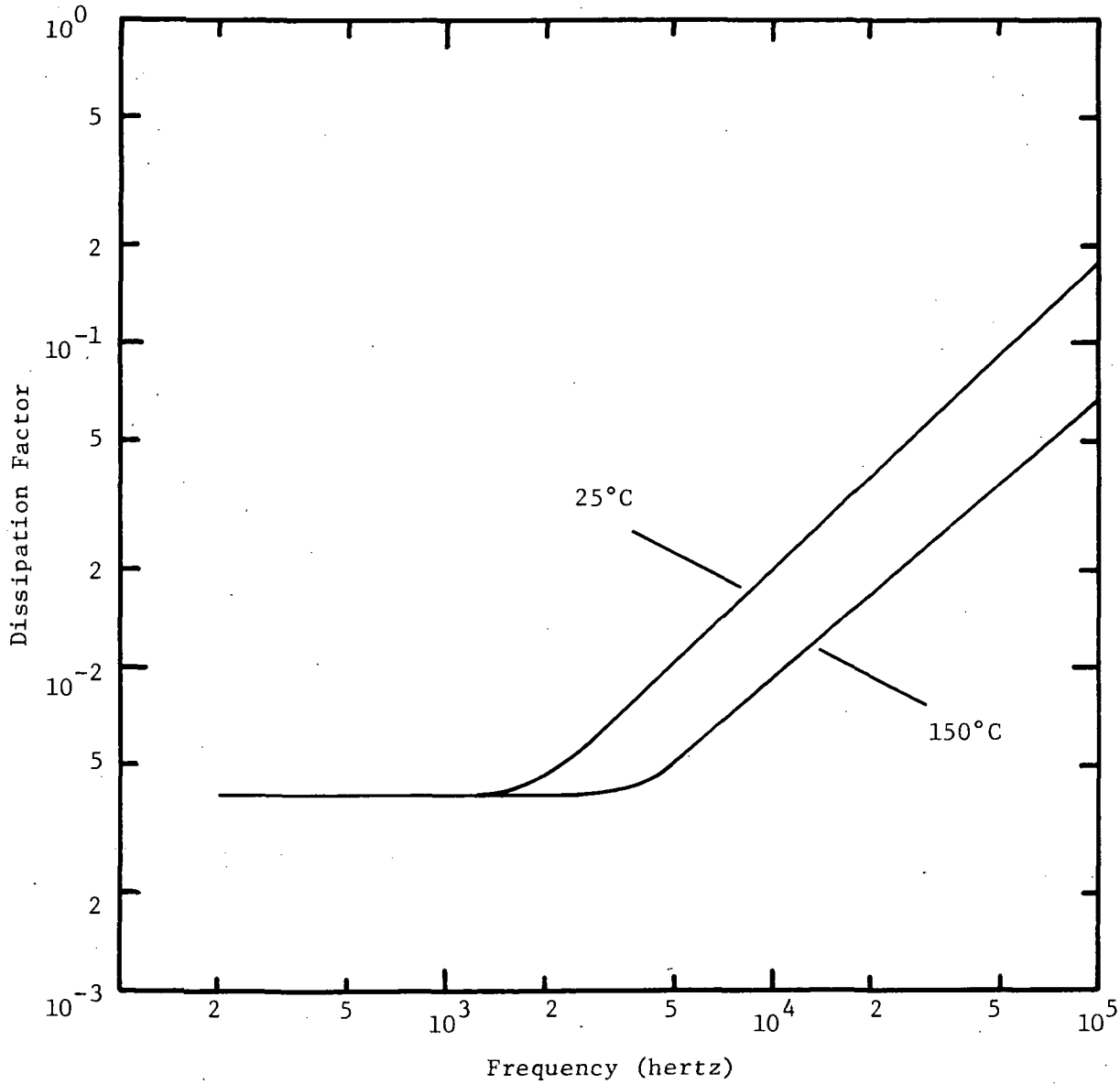

Figure 10. Dissipation Factor as a Function of Frequency at Two Temperatures for a Sixteen Layer SiO_2-Al Capacitor. The 25°C Data was Taken Before any Annealing had Taken Place

the capacitor (annealing). After some time at 150°C, the results stabilized again and yielded a smooth curve with lower dissipation factor values. Direct current leakage at the four temperatures and at 30 volts also indicated that some changes were taking place in the capacitor. These currents were 30, 27, 50, and 35 microamperes at 25°, 50°, 100°, and 150°C, respectively. These results indicate that annealing is a necessary step in the capacitor fabrication.

The next run was made with 6000 Å-thick dielectrics and resulted in two capacitors of twenty-two layers each. One capacitor failed during deposition of the 22 layer and the other failed at eight layers. The capacitances averaged 0.026 microfarads after seven layers and the dissipation factors were 0.003, 0.004, 0.003, and 0.005 at one kilohertz and approximately 25°C. After 22 layers the dissipation factor of one of the remaining two capacitors had increased sharply so the run was terminated. The other capacitor had capacitance and dissipation factor of 0.092 microfarads and 0.003, respectively, at one kilohertz and approximately 25°C. Figure 11 shows capacitance and dissipation factor for this 22 layer capacitor as functions of frequency. This capacitor was delivered to the NASA without testing its thermal stability. The lowest dissipation factor of 0.005 in air is good. However, this would probably decrease with some thermal conditioning, and the frequency range over which the dissipation factor is less than one percent would probably broaden. This would make the power dissipation of this 22 layer capacitor compare favorably with the two- and four-layer capacitors reported in Reference 4.

The energy density for the 22 layer capacitor at 40 volts was 42 millijoules per cubic centimeter of deposited material and 67 millijoules per cubic centimeter of active deposit. No capacitors were subjected to more than 100 volts dc. However, many 3000 Å-thick dielectric layers can hold 100 volts so the 6000 Å-thick dielectrics could easily have working voltages of 100 volts dc.

Test results for typical eight-layer capacitors of the smallest size studied are presented in Figures 12 and 13. Figure 12 shows the capacitance as a function of frequency and temperature. The curves for all other temperatures tested (50°, 100°, 150°, and 200°C) fall between the two curves shown. Note that the greatest effect of frequency on capacitance is 2.5 percent at 250°C. Figure 13 shows the dissipation factor as a function of frequency and temperature. Dissipation factors of less than one percent at all tested frequencies and temperatures show that these capacitors have excellent power dissipation characteristics. The energy density for these capacitors was 65 to 70 millijoules per cubic centimeter of active deposit at 40 volts.

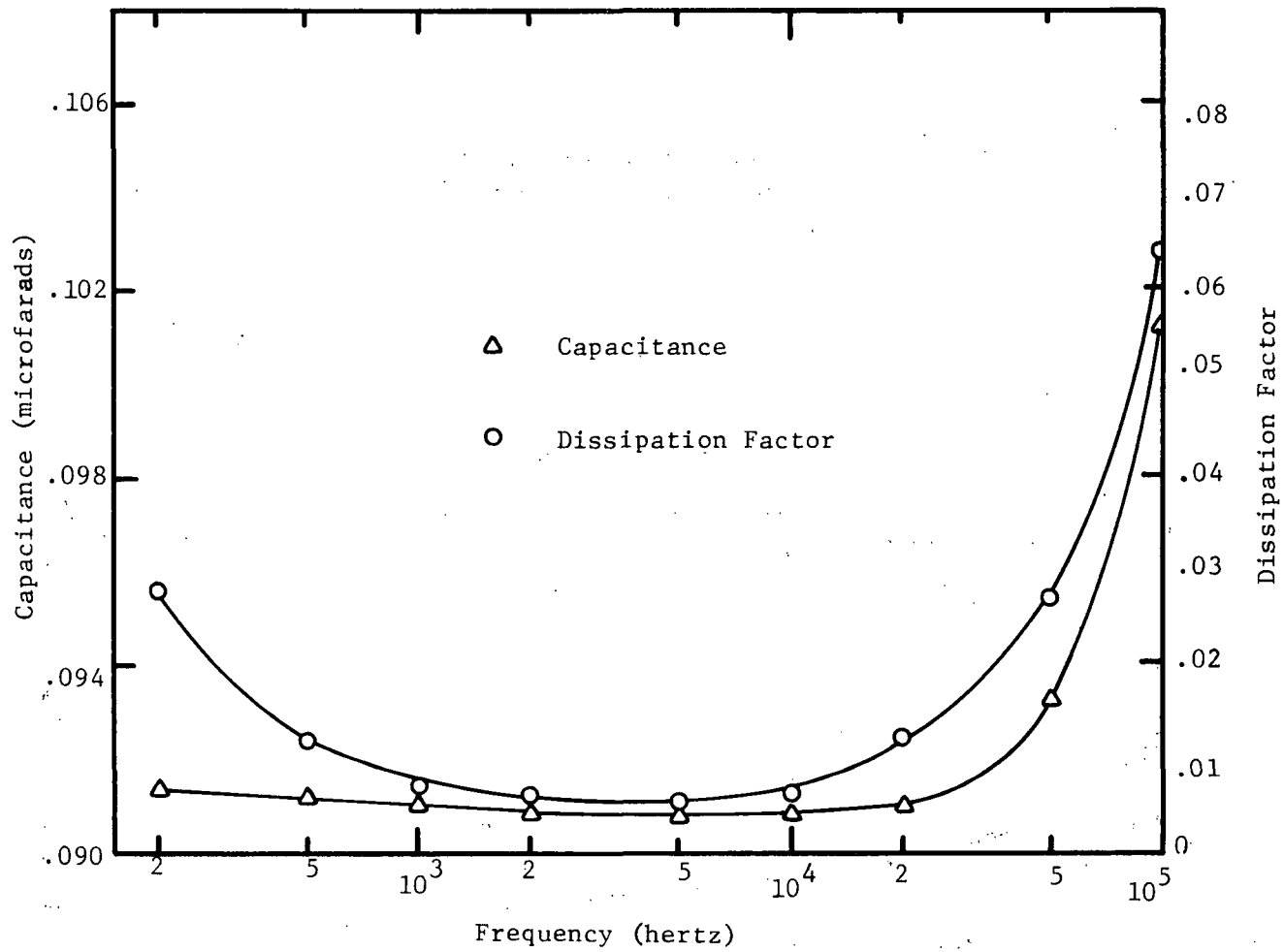

Figure 11. Capacitance and Dissipation Factor as Functions of Frequency at 25°C for a Twenty-Two Layer SiO_2-Al Capacitor.

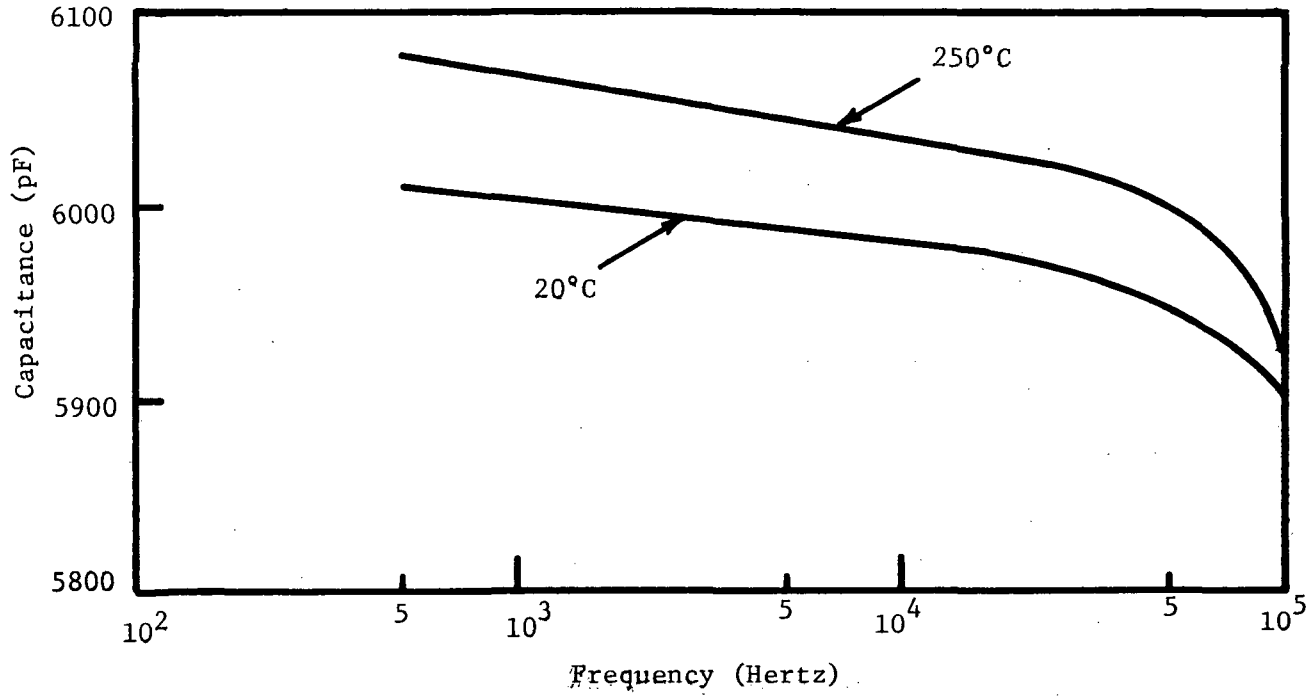

Figure 12. Capacitance as a Function of Frequency and Temperature for an Eight-Layer SiO_2-Al Capacitor.

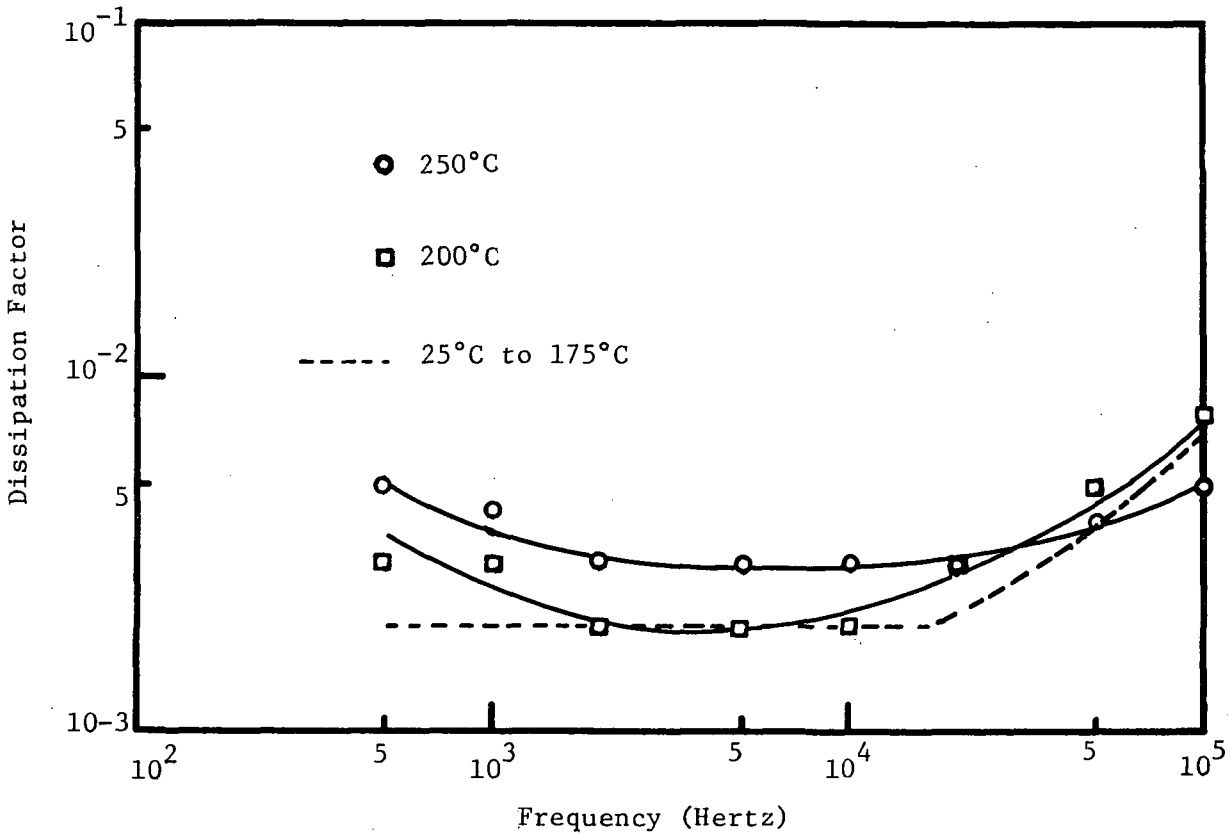

Figure 13. Dissipation Factor as a Function of Frequency and Temperature for an Eight-Layer SiO_2-Al Capacitor.

Page Intentionally Left Blank

Page Intentionally Left Blank

Page Intentionally Left Blank

APPENDIX A

Effects of Electrode Delamination

APPENDIX A

Effects of Electrode Delamination

One task of the subject contract was to investigate the feasibility of decreasing the power dissipation of the capacitors by decreasing eddy current losses in the electrodes. It was suggested that eddy currents could be curtailed by replacing solid electrodes with laminated electrodes. These laminates would be fabricated by depositing thin islands of insulating material (quartz) periodically during the course of a conductor deposition. This would require some complex masking arrangements and increase deposition times considerably. Therefore, the chances of success were evaluated before proceeding with the experimental work. There was a high probability that side effects such as the increased resistance of thinner conductors would overshadow any gain from decreased eddy currents.

Assume that a 1500 Å-thick aluminum conductor would be replaced by three 500 Å-thick aluminum layers separated by thin quartz layers. Although both cases have 1500 Å conducting thicknesses, there is more resistance in the laminate. When film thickness (d) is greater than the mean free path (l_i) of conduction electrons, the equation relating film resistivity (ρ) to bulk resistivity (ρ_0) is:

$$\rho/\rho_0 = 1 + 3/8k$$

where $k = d/l_i$. Assigning a value of 380 Å as the mean free path in aluminum (Reference 5) at room temperature yields results for 1500 Å- and 500 Å-thick aluminum as follows:

$$\text{1500 Å aluminum:} \quad \rho/\rho_0 = 1.095$$

$$\text{500 Å aluminum:} \quad \rho/\rho_0 = 1.285$$

Thus, the resistivity of 500 Å-thick aluminum films of 1.285/1.095, or 1.17 times greater than that of 1500 Å thick aluminum films. The resistance of three 500 Å thick aluminum films separated by insulating layers would be 17 percent higher than the resistance of one 1500 Å thick aluminum film assuming films with planar surfaces. In fact, deposited films have microscopically rough surfaces. On a multilayer capacitor, this roughness increases with the number of layers and becomes significant compared to the total film thickness, especially for 500 Å-thick films. At that point, the resistance of three 500Å-thick aluminum layers in a laminate becomes even greater compared to one 1500 Å-thick layer. This increased resistance in laminated electrodes will cause an increased dissipation factor at high frequency, opposing and probably overshadowing, any improvement caused by decreasing eddy current losses. These factors indicate that laminating the electrodes is probably not a feasible way of decreasing the dissipation factor. It has questionable value technically and it is very expensive.

Page Intentionally Left Blank

REFERENCES

1. Jorgenson, G.V., and Graves, W.H., *Research Into the Feasibility of Thin Metal- and Oxide Film Capacitors*, NASA CR-72779, March 1971.

2. Vromen, B.H., and Gerstenberg, D., *Proc. 1968 IEEE Electronic Components Conference*, p. 145 (May 8-10, 1968).

3. Pitt, K.E.G., *Vacuum, 17*, No. 10, p.560 (October 1967).

4. Anderson, D.C., *Research/Development, 19*, p. 46 (January 1968).

5. Chopra, K.L., *Thin-Film Phenomena*, McGraw-Hill, 1969.

DISTRIBUTION LIST

Final Report

Contract Number NAS 3-14373

National Aeronautics and Space Administration
Lewis Research Center
21000 Brookpark Road
Cleveland, Ohio 44135
Attn: N. T. Musial
M.S. 500-311 (1)

Library
M.S. 60-3 (2)

J. R. Danicic
M.S. 500-313 (1)

J. A. Kish
M.S. 54-4 (20)

J. F. Been
M.S. 54-4 (1)

G. R. Sundberg
M.S. 54-4 (1)

I. T. Myers
M.S. 54-4 (1)

B. L. Sater
M.S. 54-4 (1)

P. A. Thollot
M.S. 54-4 (1)

H. W. Plohr
M.S. 54-1 (1)

R. E. English
M.S. 500-201 (1)

Report Control Office
M.S. 5-5 (1)

National Aeronautics and Space Administration
Scientific & Technical Information Facility
P. O. Box 33
College Park, MD 20740
Attn: Acquisitions Branch (10)

National Aeronautics and Space Administration
Washington, D. C. 20545
Attn: RP/W. H. Woodward (1)

RPM/P. T. Maxwell (1)

Library (1)

National Aeronautics and Space Administration
Goddard Space Flight Center
Greenbelt, Maryland 20771
Attn: F. C. Yagerhofer (1)

C. M. MacKenzie (1)

Library (1)

National Aeronautics and Space Administration
Langley Research Center
Hampton, Virginia 23365
Attn: Mr. Merton Sussman
Building 1201
M.S. 472 (1)

Library (1)

Lyndon B. Johnson Space Flight Center
Houston, Texas 77501
Attn: Mr. F. E. Eastman
Code EB3 (1)

Mr. W. E. Rice
Code EP5 (1)

Library (1)

NASA-George C. Marshall Space Flight Center
Huntsville, Alabama 35812
Attn: Mr. R. Boehme
Code PD-DO-EP (1)

Mr. Robert Aden
Code S&E-ASTR-E (1)

Library (1)

NASA-John F. Kennedy Space Center
Kennedy Space Center, Florida 32899
Attn: Library (1)

Jet Propulsion Laboratory
4800 Oak Grove Drive
Pasadena, California 91103
Attn: Mr. Hubert M. Wick
Space Power Section (1)

Mr. Alden Schloss
Building 198/220 (1)

Mr. T. Macie
Building 122/123 (1)

Library (1)

National Aeronautics and Space Administration
Ames Research Center
Moffett Field, California 94035
Attn: Library (1)

Flight Research Center
Edwards, California 93523
Attn: C. T. Johnson, Code A (1)

Library (1)

Naval Air Systems Command
AIR 53682
Department of Navy
Washington, D. C. 20360
Attn: Mr. E. White (1)

Naval Air Development Center
Warminster, Pa. 18974
Attn: Mr. J. Segrest, AETD (1)

Naval Air Test Center
Patuxent River, Maryland 20670
Attn: Mr. T. P. Wilson, WST (1)

USAECOM
AMESEL-KL-PG
Fort Monmouth, New Jersey 07703
Attn: Mr. Frank J. Wrublewski (1)

Mr. Robreski (1)

SEPO
Division of Space Nuclear Systems
Washington, D. C. 20545
Attn: Mr. Gerald Leighton (1)

Commanding Officer
U. S. Army MERDC
Systems Application Division
SMEFB-BD
Fort Belvoir, Virginia 22060
Attn: Mr. L. Gaddy, Jr. (1)

Mr. George Sherman (APIE)
Chief, Aerospace Power Division
Air Force Aero Propulsion Lab
Wright Patterson Air Force Base
Ohio 45433 (1)

Mr. Richard L. Verga
AIPE-2
Aero Propulsion Laboratory
Wright Patterson Air Force Base
Ohio 45433 (1)

Mr. B. J. Wilson, Code 5222
Naval Research Laboratory
Washington, D. C. 20390

Naval Facilities Engr. Command
Nuclear Power Division
Washington, D. C. 20390
Attn: Mr. E. Morris Howard (1)

Mr. Myron Lowe, Code SS310
Federal Aviation Agency
800 Independence Ave., S.W.
Washington, D. C. 20553 (1)

Mr. Robert C. Hamilton
IDA-Room 19, 9th Floor
400 Army-Navy Drive
Arlington, Virginia 22202 (1)

Naval Air Systems Command
AIR 5335
Department of the Navy
Washington, D. C. 20360
Attn. Mr. Ohil Binderman (1)

Mr. Jacob A. Adams
ASBEP USAF
Wright Patterson Air Force Base
Ohio 45433 (1)

Mr. L. Cobb
AETD, AEE Division
Naval Air Development Center
Warminster, Pennsylvania 18974 (1)

Mr. E. Ward
High Speed Ground Transportation
Federal Railroad Administration
Department of Transportation
Washington, D. C. 20553 (1)

Mr. Opeka
Chief, Electro/Mechanical Branch
SM-140
800 Independence Avenue, S. W.
Washington, D. C. 20553 (1)

National Institutes of Health
Physical Sciences Administrator
Bethesda, Maryland 20014
Attn: Mr. Roger S. Powell (1)

TRW Systems Group
One Space Park
Redondo Beach, California 90278
Attn: Mr. A. D. Schoenfeld (1)

VARO
Static Power Division
1600 Dallas North Parkway
Plano, Texas 75074
Attn: Mr. W. L. McNair (1)

Engineered Magnetics
13041 Cerise Avenue
Hawthorne, California 90250
Attn: Mr. B. McComb (1)

Airesearch Mfg. Co.
2525 West 190th Street
Torrance, California 90509
Attn: Mr. K. M. Chirgwin (1)

Hamilton Standard
Electronics Dept.
Windsor Locks, Connecticut 06096
Attn: Mr. R. E. Sullivan (1)

Consolidated Avionics
800 Shames Drive
Westbury, New York 11590
Attn: Mr. G. O'Sullivan (1)

Dr. F. Storm
General Electric Co.
Research and Development Center
P. O. Box 8
Schenectady, New York 12301 (1)

Mr. V. J. Wattenburger
General Electric Co.
UFSTC
Box 8555 (1)
Philadelphia, Pennsylvania 19101

Mr. Glen Rose
Grumman Aerospace
Air Systems Div. 662
Bethpage, L. I., New York 11714 (1)

Mr. Henry Johnson
AC Electronics
Defense Research Lab.
GM Corporation
6767 Hollister Avenue
Goleta, California 93107 (1)

Mr. O. H. Preston
Unit 251780
L. T. V. Aerospace
P. O. Box 5907
Dallas, Texas 75222 (1)

Comsat Laboratories
Communications Satellite Corp.
Box 115
Clarksburg, Maryland 20734
Attn: Mr. Esch
Spacecraft Lab. (1)

Mr. Esrom Day
Fairchild Hiller
Space & Electronic Systems Div.
Fairchild Drive
Germantown, Maryland 20767 (1)

Mr. Lionel Boulet
Director, Hydro-Quebec
Research Institue
c/o Hydro Quebec
Montreal, Canada (1)

Dr. A. E. Fitzgerald
Dean of Faculty
Northeastern University
360 Huntington Avenue
Boston, Massachusetts 02115 (1)

Dr. H. H. Woodson
Professor of Electrical
Engineering
Massachusetts Institute of
Technology
Cambridge, Massachusetts 02139 (1)

Dr. Chauncey Starr
Dean of Engineering
University of California
Los Angeles, California 90009 (1)

Hughes Aircraft Co.
Imperial Highway
El Segundo California 90245
Attn. Mr. W. E. Michel
Dept. 22-28-00, Bldg. 366
M/S522 (1)

Philco Ford Corporation
3825 Fabian Way
Palo Alto, California 94303
Attn: R. J. Grant, Space
Power & Propulsion (1)

Sperry Rand
Space Support Div.
716 Arcadia
Huntsville, Alabama 35801
Attn: W. F. Wrye (1)

Westinghouse Electric Corp.
Aerospace Electrical Div.
Lima, Ohio 45802
Attn: Mr. H. James (1)

Dr. Karl Martinez
Boeing Company
P. O. Box 3868
Seattle, Washington 98124 (1)

Mosher C. Clifford
Edison Electric Institute
3221 Walnut Street
Philadelphia, Pennsylvania 19104 (1)

Dr. A. H. B. Walker
Westinghouse Electric Corp.
Research Center
Beulah Road
Pittsburgh, Pennsylvania 15235 (1)

Prof. Thomas G. Wilson
Duke University
School of Electrical Engineering
Durham, North Carolina 27707 (1)

Arthur D. Little, Inc.
Acorn Park
Cambridge, Massachusetts 02140
Attn: Mr. L. Stratton (1)

North American Rockwell Corp.
Los Angeles Div.
International Airport
Los Angeles, California 90009
Attn: Mr. J. Pierro (1)

Dr. Victor Wouk
Gulton Industries
212 Durham Avenue
Metuchen, New Jersey 08840 (1)

Raytheon Company
Sorensen Operation
South Norwalk, Connecticut 06854
Attn: Mr. P. Muchnick (1)

Howard B. Hamilton
108 Pennsylvania Hall
University of Pittsburgh
Pittsburgh, Pennsylvania 15213 (1)

Honeywell, Inc.
600 Second Street, North
Hopkins, Minnesota 55343
Attn: Mr. J. Lingle (1)

Power Information Center
University of Pennsylvania
3401 Market Street, Room 2107
Philadelphia, Pennsylvania 19104 (1)

Space Technology Laboratories, Inc.
One Space Park
Redondo Beach, California 90278
Attn: Mr. D. Glaser (1)

IIT Research Institute
10 West 35th Street
Chicago, Illinois 60616
Attn: Mr. J. Radnick (1)

Wilmore Electronics Co.
P. O. Box 2973
West Durham Station
Durham, North Carolina 27705 (1)

Lear Siegler, Inc.
Power Equipment Division
P. O. Box 6719
Cleveland, Ohio 44101
Attn: Mr. R. Dickman (1)

Vapor Corporation
Vap-Air Division
Box 533
Warehouse Point, Connecticut 06088
Attn: Mr. B. E. Butenkoff (1)

Professor R. G. Holf
University of Missouri
College of Engineering
Columbia, Missouri 65201 (1)

Bendix Corporation
9 Meriam Street
Lexington, Massachusetts 02173
Attn: Mr. Charles E. Rukstuhl (1)

Westinghouse Electric Corporation
Lima, Ohio 45802
Attn: Mr. Dwayne Rife (1)

General Electric Company
Wynesboro, Virginia 22980
Attn: Mr. D. L. Plette (1)

Sundstrand Aviation
4747 Harrison Avenue
Rockford, Illinois 61108
Attn: R. C. Baker (1)

General Electric Company
Technical Center
Philadelphia, Pennsylvania 19101
Attn: Mr. Archie R. Ruggieri (1)

Bose Corporation
17 Erie Drive
Natick, Massachusetts 01760
Attn: Dr. A. Bose (1)

Hewlett Packard
620 Page Mill Road
Palo Alto, California 94303
Attn: Dr. Richard Soshes (1)

United Airlines, Inc.
Engineering Department
International Airport
San Francisco, California 94128
Attn: Mr. James A. Aldrich (1)

Boeing Aircraft Corporation
Commercial Airplane Division
P. O. Box 3733
M.S. 4199
Seattle, Washington 98124
Attn: Mr. Lewis Weiner (1)

Lockheed, California Company
Building 170 B1
Burbank, California 91503
Attn: Mr. M. J. Cronin (1)

American Airlines
Maintenance & Engineering Department
Tulsa, Oklahoma 74151
Attn: Mr. R. C. Munroe (1)

Mr. Robert C. Sprague
Sprague Electric Company
North Adams, Massachusetts 01890 (1)

Mr. W. O. Fleckenstein
Western Electric
Princeton, New Jersey 08540 (1)

Mr. Lionel Boulet
Director, Research Institute
Quebec Hydroelectric Commission
75 Dorechester West
Montreal, P. Q., Canada (1)

Dr. S. D. T. Robertson
University of Toronto
Department of Electrical
Engineering
Toronto, Canada (1)

Dr. Lester van Atta
Assistant Dean of Engineering
University of Massachusetts
Amherst, Massachusetts 01002 (1)

Professor G. D. Sheckels
Chairman, Electrical Engineering
University of Massachusetts
Amherst, Massachusetts 01002 (1)

Dr. M. R. Donaldson
Chairman
Department of Electrical Engineering
University of South Florida
Tampa, Florida 33620 (1)

Dr. Shirley A. Johnson, Jr.
Director, Denver Research Institute
University of Denver
Denver, Colorado 80210 (1)

Dr. F. C. Schwarz
18839 Timber Lane
Fairview Park, Ohio 44126 (1)